Measuring the EHD Film Thickness in a Rotating Ball Bearing

Peter Ward*, Alan Leveille* and Peter Frantz*

Abstract

This paper presents two independent ways to directly measure the change in axial deflection of a bearing that is proportional to the magnitude of the total elastohydrodynamic (EHD) film developed. The first uses multiple capacitance displacement gages as a direct measurement of axial displacement and the second method uses the change in operating preload force to calculate the axial change in the test fixture and bearing stack. Convergence of the results from two independent techniques adds confidence to the experimental process. Either method can provide accurate EHD film thickness over extended time for a complete bearing under varying load, speed and lubrication conditions. Additionally, the methods are equally applicable to non-metallic materials, such as Si_3N_4 balls, which preclude the use of other techniques. The method has some advantages to the practicing engineer over the classical ball on a flat quartz plate because the full range of bearing design parameters and kinematic interactions are operating.

The EHD film thicknesses of two oils and one grease were measured in an operating 304 sized angular contact bearing for up to 600 hours of running time at 6000 rpm. EHD film thickness was determined by simultaneously measuring the resultant displacement and axial force change of the outer rings due to collapse of the EHD film when the bearing pair was brought from full speed to rest. Because each measurement of axial displacement was completed within 2 seconds, the results are not affected by a contribution due to thermal expansion. We compared a common synthetic hydrocarbon base oil (Pennzane) with a common mineral oil (Coray). We found the synthetic oil film thickness to be approximately one half that of the mineral oil. We also compared film thickness with both large and small amounts of grease. We found that the large grease amount produced a prolonged run-in transient film that was thicker than the base oil steady state film. However, with a smaller amount of grease, the thickness fell to a value that was comparable to the base oil. Initial assessment indicates that the degree of lubricant starvation is greater than can be accounted for with conventional EHD theory.

Introduction

Ball bearings in numerous aerospace mechanisms are lubricated with a single charge of grease or oil that is expected to last on the order of 10 years. Development and maintenance of an elastohydrodynamic (EHD) film that is sufficient to prevent wear is dependent upon application conditions, bearing design and lubricant properties. As demands on lubricant performance grow, lubricant conditions are pushed towards a deeply starved regime where conventional models of EHD film thickness break down [1]. Therefore, our experimental and theoretical tools for demonstrating lubricant performance for a given application are becoming increasingly compromised. For this reason, we devised an experimental approach to measure EHD film thickness of an operating pair of bearings with two objectives. The first is to directly measure the film thickness in applications of immediate relevance to specific flight requirements to ensure an adequate film is present. The second is to evaluate the validity of modern lubricant starvation models and to adapt them for use in design of aerospace applications. This presentation is intended to be an introduction and demonstration of the experimental technique.

The experimental procedure presented here provides an accurate measure of the time dependent EHD film thickness behavior. The magnitude of the EHD film in a bearing is proportional to the change in the axial stick-out (end play) of the bearing between a condition of running at speed with an EHD film and a condition of zero RPM with no EHD film. This change in end play was experimentally determined simultaneously with two independent techniques. The first was to measure it directly using air-gap

* The Aerospace Corporation, El Segundo, CA

capacitance displacement gages. The second way was to deduce it by combining the measured spring rate of the test rig in series with the calculated spring rate of the two bearings and then calculating what the axial change in deflection had to be to account for a measured axial force change between running with an EHD film and zero RPM with zero EHD film. The concurrence of these two methods provides a way of validating that the test set-up is correct for any given test. The measurement of axial change is similar in principle to the method of Tyler, et al [2]. However, our approach introduces a nearly isothermal measurement that eliminates the very significant effect of temperature on the measured change in axial stickout. To illustrate the importance of temperature, for steel parts and a 15-degree operating contact angle, a 1-degree F uncertainty in temperature across the bearing results in a measured stickout change of 34 micro-inches for the 304 size bearing reported herein. This uncertainty is much larger than the actual EHD film thickness.

Several other techniques for measuring film thickness in an operating rolling contact bearing have been described in the literature. Measurements of acoustic emission have been used to record the noise created by asperity contacts between the balls and races [3]. This technique is well suited for in-situ monitoring of real bearing applications, but does not provide a direct quantitative measure of the film thickness and loses resolution when the film thickness grows beyond 3 times the composite surface roughness. The electrical capacitance and resistance across the bearing has been used to infer the EHD film thickness [4,5]. However, the inferred film thickness is often dependent on uncertain estimates of several properties, such as the oil volume outside the contact, the size and shape of the contact, and the dielectric properties of the material between the surfaces. Ultrasonic reflection [6] is a promising new technique, but it is challenging to produce sufficient resolution under the relevant speed conditions. Furthermore, it measures only the film between the ball and outer race and not the inner race, which is often more deeply starved.

Analytical Method

As the film between the ball and races grows, the inner ring is forced to deflect with respect to the outer ring, resulting in a change in stick-out. To analyze the geometric situation, the increased film thickness is modeled as an increase in the overall ball diameter. Figure 1 shows the change in inner ring position caused by the hypothetical increase in the ball diameter. Figures 1A and 1B each show the cross section of an outer ring, ball, and inner ring, from top to bottom. Figure 1A represents the bearing with no lubricant film between the ball and race, such as would occur when the bearing is at rest. Figure 1B

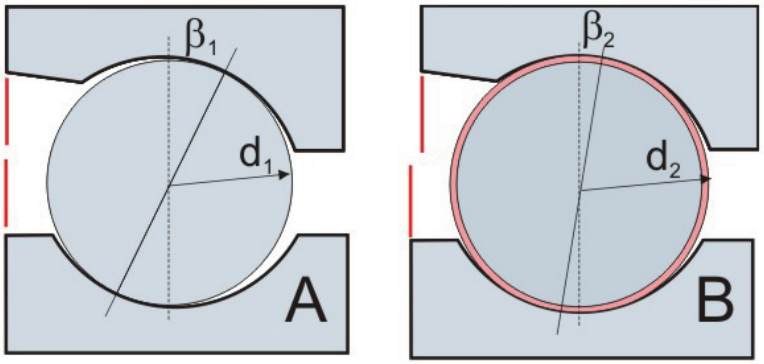

Figure 1. Cross section of a bearing raceway/ball contact at rest (A) and with a hypothetical lubricant film surrounding the ball (B).

shows the high-speed bearing, with the appearance of a lubricant film as a ring surrounding the ball. This film is shown with uniform thickness around the ball only for the purpose of illustration. The inner ring deflects to the left and the contact angle is reduced. The inner ring deflection is equal to one half of the change in end play of the bearing resulting from a change in the effective diameter of the ball. Additional deflection due to elastic deformation of the balls and races has also been accounted in our model. Details of the technique and results of our film thickness measurements are described below.

The end play of the bearing shown in Figure 1A (P_{E1}) is related to the ball diameter (d_1) by the following relationship:

$$P_{E1} = 2B_1 d_1 \sin \beta_1 \qquad \text{Eq (1)}$$

Where B_1 is the total curvature for the bearing in Figure 1A, given by:

$$B_1 = \frac{r_o}{d_1} + \frac{r_i}{d_1} - 1 \qquad \text{Eq (2)}$$

Where r_o is the inner ring radius and r_i is the inner ring radius.

Similar relationships may be written for the bearing shown in Figure 1B, with the subscript 2 substituted for 1. For each experimental data point, the change in end play ($\Delta P_E = P_{E1} - P_{E2}$) is measured with the techniques described below. The full-speed contact angle β_2 is measured by observing the ratio of the shaft rotational frequency to the ball group rotational frequency. The total film thickness, the sum of the inner and outer ring EHD films, is given by $d_2 - d_1$. Solving from equation 3, the total film thickness is given by:

$$d_2 - d_1 = \frac{2B_1 d_1 \sin \beta_1 - \Delta P_E}{2B_2 \sin \beta_2} - d_1 \qquad \text{Eq (3)}$$

Although this technique provides a quantitative measure of the sum of the inner and outer film thicknesses, it gives no information that allows one to discern how much of that sum is due to each interface. An approximate ratio can be obtained through the application of conventional EHD film thickness analytical methods [7]. This approach was used here to demonstrate that the film thickness at the inner ring is approximately 40% of the total, and the film thickness at the outer ring is the remaining 60%. Therefore, in our final analysis will treat the inner ring film thickness as being approximately 40% of the total film thickness.

Experimental Method

A pair of 304 sized bearings is mounted in a face-to-face (DF) configuration inside a steel housing, as shown in Figure 2. A single pair of hybrid bearings, with CRU20 rings, Si3N4 balls and a phenolic cage, was used for all experiments shown here. The preload force is both applied and measured using a compliant, ring-shaped load cell compressed between the lower bearing and the cartridge. A spacer separates the outer ring of the lower bearing from the load cell. To simplify alignment, the load cell bears on the housing through a ball-in-cone arrangement. Preload is set by screwing the upper and lower housing halves together. The upper end of the shaft is attached to a high-speed precision spindle that rotates the inner rings. The entire assembly hangs from the motor spindle by a connection to the shaft. The housing and outer rings are prevented from rotating by a lever arm (not shown) that bears on a second load cell to measure bearing drag torque.

In this arrangement, the outer ring of the upper bearing is stationary with respect to the housing, while the outer ring of the lower bearing translates axially through a distance equal to the sum of the two bearing displacements. Since the motion of each outer ring is equal to half of the change in end play, the total measured axial translation of the outer ring of the lower bearing (the sum of both bearings) is equal to the total change in end play of each bearing, ΔP_E. The bearing test cartridge is instrumented with sensors to detect displacement of the outer ring and changes in the operating preload. These sensors provide the change in end play that is used to determine film thickness with the “load change method” and the “air gap displacement method” described below.

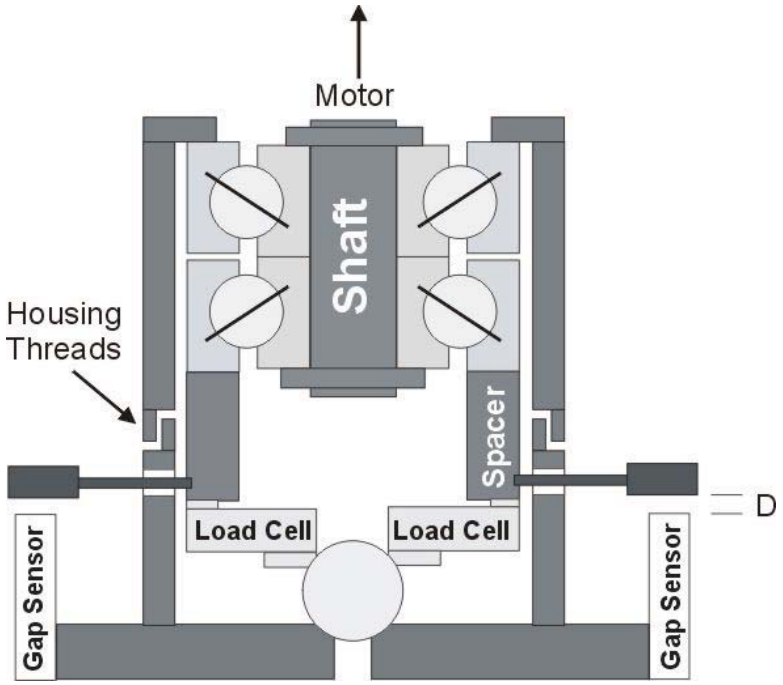

Figure 1. Schematic of the bearing test facility, not shown to scale.

Load change method

The first method to detect the change in end play uses the change in bearing preload from the load cell shown in Figure 2. The displacement of the outer ring is equal to the measured change in load times the yield rate of the bearing cartridge system, as shown in equation 4:

$$\Delta P_E = \Delta T \times Y_{system} \qquad \text{Eq (4)}$$

Where $\Delta T = T_2 - T_1$ is the measured axial thrust load change in lbs, and Y_{system} is the sum of contributions to the axial yield rate from the two test bearings and the test fixture in μin/lb. The yield rate of the bearing pair was determined using computational bearing analysis tools (DYBA). The bearing pair yield rate takes into account the change in bearing deflection due to elastic deformation at the Hertzian contact. The yield rate of the system was determined through experimental calibration by directly measuring the displacement for a given force.

The signal from this load cell is collected by a data acquisition system in real time during the bearing test. To avoid uncertainties in the outer ring position due to thermal fluctuations, the film thickness measurements reported here were determined from the nearly instantaneous change in end play when the bearing rapidly decelerated from full speed to rest. When the full speed and zero speed data points are collected nearly coincidentally in time, there is no period in which the temperatures can drift to cause thermal changes in the end play. An example of a test data collection sequence is shown in Figure 3. The data stream nearest to the top of this chart shows axial force measured by the load cell. Each of the three disturbances seen in this data are stop/start cycles during which the bearing deflection was measured. The full speed thrust load (T_2) was chosen as the data point immediately before stopping the bearing, and the zero speed load (T_1) was chosen as the data point immediately after the bearing came to rest. During each restart, we observe an overshoot transient due to slumping of the lubricant at rest and the subsequent redistribution after start-up. The difference between these two values is taken as the change in axial load (ΔT) to be used in equation 4. One drawback to this technique is that each time the bearing is stopped, the lubricant distribution is reset. This will tend to prolong the run-in period, and may cause the measured film thicknesses for a given amount of running time to appear thicker than they would if the bearing had no interruption of use.

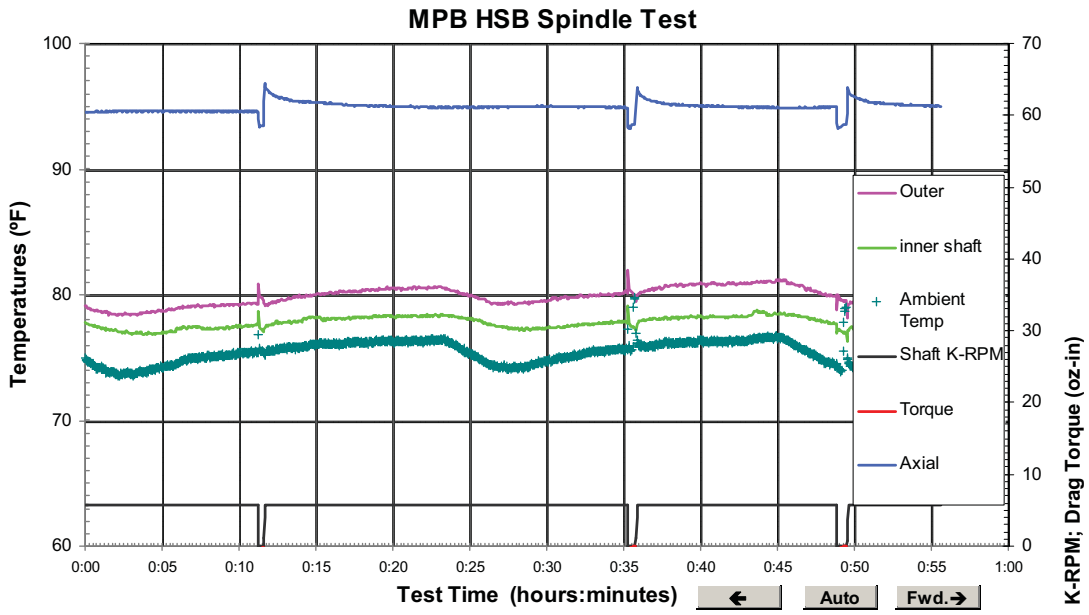

Figure 3. An example of raw data. The top data stream shows the axial load that is used to determine bearing deflections. The three data streams bundled near the center are, from top to bottom, temperatures of the outer ring, inner ring, and laboratory ambient.

Air gap displacement change method

The total axial deflection of the outer ring is directly measured as the deflection of reference paddles ($\Delta D = D_2 - D_1$) connected to the spacers that move with the outer rings, as shown in Figure 2. The axial position of these paddles is monitored with non-contact proximity (air gap) sensors. To eliminate uncertainties due to run-out of the bearing system, the response from a pair of paddles mounted on opposite sides is averaged to produce the total change in axial position. To convert this total change in axial position into a change in the bearing end play for use in equation 3, one must first correct for the displacement due to yield rate of the bearing pair.

To determine the contribution due to the yield rate of the bearing pair, let:

h_1 = axial deflection of a single row at thrust load T_1
h_2 = axial deflection of a single row at thrust load T_2
f_1 = change in stick-out of a single row due to the EHD film at zero speed = 0
f_2 = change in stick-out of a single row due to the EHD film at full speed

The axial positions given by the air gap sensor may be written as:

$$D_2 = 2(-h_2 + f_2) \qquad \text{Eq (5a)}$$
$$D_1 = 2(-h_1 + f_1) \qquad \text{Eq (5b)}$$

Or:

$$\Delta D = D_2 - D_1 = -2h_2 + 2h_1 + 2f_2 \qquad \text{Eq (6)}$$

So that:

$$2f_2 = \Delta D + 2(h_2 - h_1) \qquad \text{Eq (7)}$$

The quantity $2f_2$ is then taken as the change in end play (ΔP_E) to be used in equation 3. The quantity (h_2-h_1) is equal to the product of the measured change in thrust load and the yield rate of a single bearing. As mentioned above, this yield rate is determined using computational bearing analysis tools (DYBA). Since

this quantity adds to the capacitance measurement distances, the resulting EHD is larger than if this correction were not used.

Results and Discussion

Coray vs. Pennzane Oil

When reviewing the results shown below, bear in mind that these film thickness results apply only to this specific set of bearing geometry, materials and operational conditions. Each experiment shown here was performed with the same pair of 304 sized angular contact bearings operating at 6000 rpm.

The first experiments described here were designed to determine the time scales for run-in, and the final absolute film thicknesses, of two base oils that have been commonly used in aerospace applications. In each case, approximately 20 mg of the base oil, formulated with TCP, was added with a clean syringe to each row. This quantity was sufficient to show a meniscus at each ball/race interface at 10X. The bearings were then operated at 6000 rpm. At periodic intervals during the run-in, bearing operation was halted to measure the film thickness. At each interruption, film thickness was recorded and the speed was returned to 6000 rpm.

Results of these experiments are shown in Figure 4, where the open symbols represent Coray and the filled symbols represent Pennzane. In both cases, the triangles represent data collected with the load cell and the circles represent data collected with the displacement sensors. First of all, we find excellent agreement between the two independent techniques for measuring deflection of the rings. Second, we

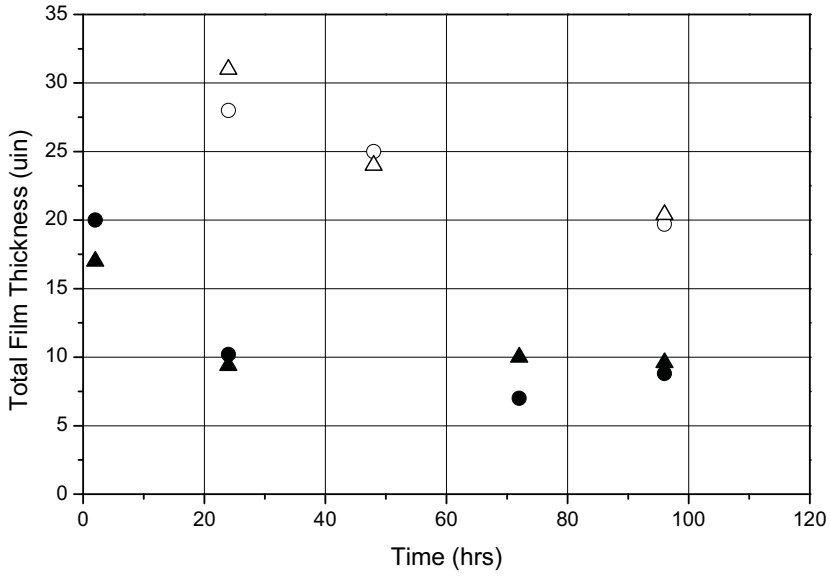

Figure 4. Total Film thickness (in microinches) as a function of cumulative time operating at 6000 rpm with neat base oils formulated with TCP. Open symbols represent Coray and filled symbols represent Pennzane. Triangles are the results from the load cell and circles are the results from the displacement sensors.

find that the run in of Pennzane was nearly complete after only 24 hours, while the Coray took significantly longer. Third, after 96 hours of cumulative use, the film thickness of Coray was more than twice that of the Pennzane. More significantly, the total film thickness for Pennzane at the contact between the ball and inner ring was very small. Using the Hamrock-Dowson expression [7] to determine the partitioning of the film between the inner and outer races, we find that 40% of the film is at the inner ring and 60% is at the outer. This implies that the inner ring film thickness is approximately 3.6 μin after

only 24 hours of operation. Since the composite surface roughness for the test articles is approximately 2.0 μin, the nominal operating condition provides a film that is under 3 times the composite roughness.

The fully flooded total film thickness (the sum of the inner and outer) predicted by the Hamrock-Dowson expression [7] is 132 μin for Pennzane. With the conventional Coy-Zaretsky starvation reduction factors [8,9], this prediction falls to approximately 77 μin for Pennzane. Our measurements show ~9 μin total film thickness after 24 hours. It is evident that our films are much more deeply starved than predicted by the Coy-Zaretsky analysis. The primary reason for this discrepancy is that the Coy-Zaretsky approach takes into account kinematic starvation, where resupply of the EHD contact is limited by rapid ball passes, but neglects deeper starvation due to a restricted amount of lubricant in the vicinity of the contact. In fact, the experiments used to validate the Coy-Zaretsky approach were performed an oil-air mist of lubricant provided to the contact [9]. Developing the ability to make quantitative estimates of this steady state film thickness with restricted lubricant supply is the subject of ongoing investigation.

Rheolube Grease Results

For the next set of experiments reported here, the bearing was cleaned and a single charge of 1.1 g Rheolube grease per row (Pennzane oil with a thickener, obtained from Nye Lubricants) was distributed throughout the ball complement. The bearing was then operated at 6000 rpm, and operation was interrupted sporadically to measure film thickness as described above. The symbols shown in Figure 5 represent the film thickness as measured by capacitance proximity sensors (circles) and load cell (triangles). The first data point was collected after the initial lubricant run-in disturbances were suppressed after 22 hours. The average value for the total film thickness from the two techniques was 19 μin. After this point, the film thickness fell to less than 17 min after 98 hours, but appeared to rise slightly to 18 μin after 365 hours.

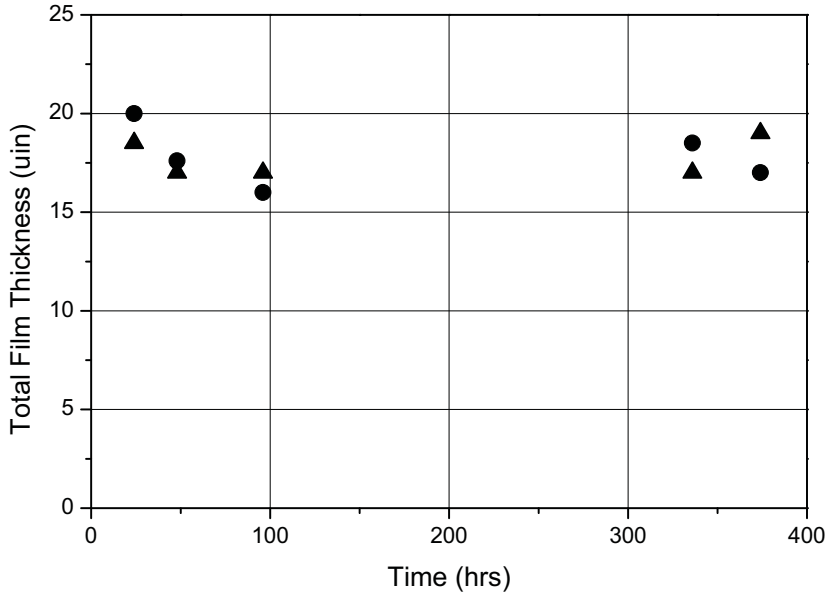

Figure 5. Total Film thickness (in microinches) as a function of cumulative time operating at 6000 rpm with a grease pack of 1.1 g Rheolube. Triangles are the results from the load cell and circles are the results from the displacement sensors.

The observation of a long-term grease film that is much thicker than the oil film contradicts many of the observations reported in the literature. Others have found that the response with grease is initially much greater during run-in, but that it falls to the oil film thickness after the run-in is complete and then it falls

further as the supply of oil from the thickener is reduced. For reasons explained below, we surmise that this indicates that our lubricant has not fully run in after 400 hours.

In the final set of experiments reported here, a thin film of Rheolube grease (0.14 gm per row) was applied to the bearing components before it was again operated at 6000 rpm. These results are shown in Figure 6. We found that the film began with a thickness that was comparable to the apparent steady state condition with the full grease pack (~19 μin). However, the film thickness was observed to fall continuously over the next 500 hours to approximately 9 μin. The final data points suggest that the rate of decline was reducing at this point, but it is unclear whether the thickness would have continued to fall below 9 μin with extended operation.

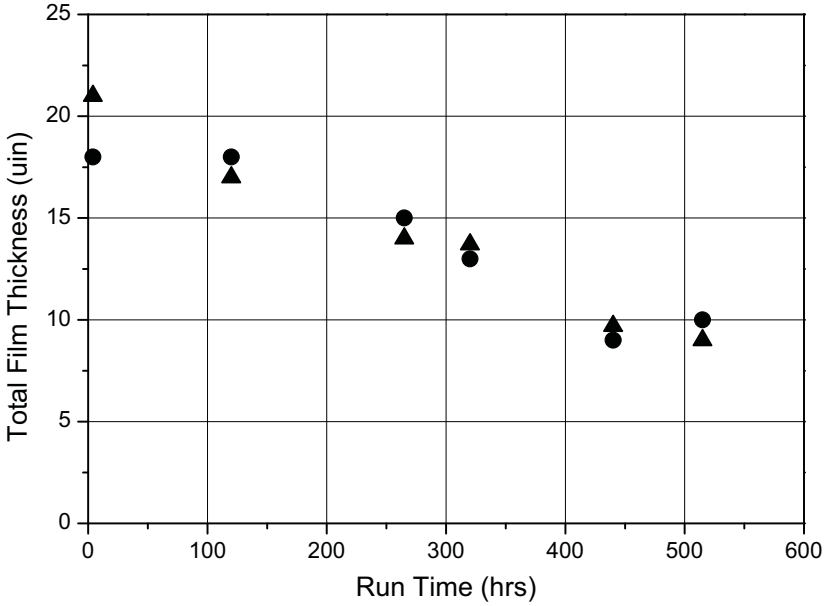

Figure 6. Total Film thickness (in microinches) as a function of cumulative time operating at 6000 rpm with a grease pack of 0.14 g Rheolube. Triangles are the results from the load cell and circles are the results from the displacement sensors.

The continued maintenance of a nearly 20 μin film thickness in Figure 5 was likely due to some prolonged retention of the grease thickener in the EHD contact. Figure 6 shows that the total film thickness will fall to 9 μin if starvation is driven further by restricting lubricant resupply. Figure 4 shows that if the film is resupplied only with neat oil, then the thickness will also fall to approximately 9 μin. We conclude that the robust film of Figure 5 must be due to some enduring intermittent resupply of grease to the contact rather than just oil. We surmise that a thin film of grease persists on the balls outside the running band, providing fresh grease to the contact when the ball spin axis is disturbed. This represents a transient condition that would likely diminish with continued operation. This run-in transient may have been artificially prolonged by a lack of disturbances to the bearing during our controlled testing. Therefore, Figure 6 suggests that the film thickness shown in Figure 5 would eventually fall to below 10 μin after prolonged use in a typical bearing application.

Conclusion

We have demonstrated a technique to measure the total EHD film thickness in an operating angular contact bearing. Excellent correspondence between the two independent methods of measuring outer ring deflection provides confidence in this measure. Our procedure for measuring the instantaneous

change in outer ring position provides excellent independence from thermally induced changes in outer ring position. We conclude that this technique is suitable for the investigation of film starvation in grease lubricated angular contact bearings.

Our initial investigation into film thickness with lubricants of immediate relevance to aerospace applications shows that the steady state Coray oil film was approximately twice that of the Pennzane oil film. Furthermore, the total Pennzane film thickness (9 μin) implies that the upper limit to the film thickness of the inner ring was 3.6 μin. This is less than three times the composite surface roughness (3 x 2 μin = 6 μin). This is also much less than the value predicted using conventional starvation analytical methods. Since the starvation analysis based upon surface tension driven resupply allows for an arbitrarily small film under certain conditions [1, 10], we will continue to pursue quantitative analysis using these techniques. However, further testing will be required to establish the oil film thickness in the vicinity of the contact (h_{oil}) before these methods can be used to produce a quantitative prediction.

Experiments with a large amount of Rheolube grease (1.1 g per row) show general agreement with other comparisons of grease and oil film thicknesses in the literature. We found that the film thickness was approximately equal to the flooded oil film thickness (before run-in), where the literature generally shows a typical grease to be slightly thicker before run-in. In contrast to the literature, however, we found that the grease film thickness did not fall appreciably during the nearly 400 hour test. We surmise that this is due to benign operating conditions that did not stimulate regular changes in ball spin axis. With prolonged periods of ball tracking, the depletion of grease from the ball surface was delayed, providing an intermittent supply of oil and thickener to the contact. This produced an extended run-in transient with a nearly 20 μin EHD film.

Experiments with a small amount of grease (0.14 g per row) show the results of a run-in that is more likely to represent the conditions of a real application. With regular disturbances in speed and/or load experienced during an actual application, the high yield stress of the grease thickener would cause channeling to the sides of the ball path on the races and more rapid depletion of thickener from the ball surface. This would approach the situation that was artificially created with the reduced initial charge of grease in this experiment. We found that the EHD film thickness fell over approximately 500 hours to approximately the same level as the oil film thickness. This also contradicts many of the results shown in the literature (for ball-on-plate interferometric film thickness instruments), which have shown a grease film thickness that is significantly reduced from the oil film thickness. However, it is possible that the film thickness in these experiments would continue to fall with continued testing.

Acknowledgements

This work was supported by The Aerospace Corporation's Independent Research and Development Program funded by the Space and Missile Systems Center (SMC) of the USAF under contract number FA8802-04-C-0001.

References

1. Cann, P.M. and Lubrecht, A.A. "An Analysis of the Mechanisms of Grease Lubrication in Rolling Element Bearings" *Lubrication Science,* 11 (1999), 227-242
2. Tyler, J.C., Carper, H.J., and Ku, P.M. "EHD Film Thickness Behavior in DMA Bearings. Part I – Experimental and Computational Techniques" *ASLE Transactions*, 22(3) (1977), 201-212
3. Miettinen, J., Andersson, P., and Wikstrom, V. "Analysis of Grease Lubrication Using Acoustic Emission Measurement" *I. Mech. E., J. Engr. Tribology,* 215 (2000)
4. Qi, G.-P. "Development and Application of the Instruments for Rolling Bearing EHL Oil Film Thickness Measurement" *Modeliing, Measurement, and Control A: General Physics and Electronics,* 73(3) (2000), 40-46
5. Zheng, W., Zhang, Z, Sun, S. "The New Development of Measuring EHL Oil Film Thickness for Thrust Bearing" *Proc. 17th IEEE Instrumentation and Measurement Technology*, vol. 3 1409-1413, IEEE, Piscataway, NJ.

6. Zhang, J., Drinkwater, B.W., and Dwyer-Joyce, R.S. “Acoustic Measurement of Lubricant Film Thickness in Ball Bearings” *J. Acoustic. Soc. Am.* 119(2) (2006), 863-871
7. Hamrock, B.J. and Dowson, D. “Isothermal Elasohydrodynamic Lubrication of point contacts, Part IV, Starvation Results” *ASME J. Lubr. Technol.* 99 (1977), 15-23
8. Chiu, Y.P. “An Analysis and Prediction of Lubricant Film Starvation in Rolling Contact Systems” *ASLE Trans.* 17 (1974), 22-35
9. Coy, J.J., and Zaretsky “Some Limitations in Applying Classical EHD Film Thickness Formulas to a High-Speed Bearing” *ASME J. Lubr. Technol.* 103 (1981), 295-301
10. Cann, P.M., Damiens, B., and Lubrecht, A.A. “The Transition between Fully Flooded and Starved Regimes in EHL” *Tribology International* 37 (2004), 859-864